

# Code Rate Optimization via Neural Polar Decoders

Ziv Aharoni, *Member, IEEE*, Bashar Huleihel, *Student Member, IEEE*, Henry D. Pfister, *Senior Member, IEEE*,  
and Haim H. Permuter, *Senior Member, IEEE*

**Abstract**—This paper proposes a method to optimize communication code rates via the application of neural polar decoders (NPDs). Employing this approach enables simultaneous optimization of code rates over input distributions while providing a practical coding scheme within the framework of polar codes. The proposed approach is designed for scenarios where the channel model is unknown, treating the channel as a black-box that produces output samples from input samples. We employ polar codes to achieve our objectives, using NPDs to estimate mutual information (MI) between the channel inputs and outputs, and optimize a parametric model of the input distribution. The methodology involves a two-phase process: a training phase and an inference phase. In the training phase, two steps are repeated interchangeably. First, the estimation step estimates the MI of the channel inputs and outputs via NPDs. Second, the improvement step optimizes the input distribution parameters to maximize the MI estimate obtained by the NPDs. In the inference phase, the optimized model is used to construct polar codes. This involves incorporating the Honda-Yamamoto (HY) scheme to accommodate the optimized input distributions and list decoding to enhance decoding performance. Experimental results on memoryless and finite state channels (FSCs) demonstrate the effectiveness of our approach, particularly in cases where the channel’s capacity-achieving input distribution is non-uniform. For these cases, we show significant improvements in MI and bit error rates (BERs) over the ones achieved by uniform and independent and identically distributed (i.i.d.) input distributions, validating our method for block lengths up to 1024. This scalable approach has potential applications in real-world communication systems, bridging theoretical capacity estimation and practical coding performance.

**Index Terms**—Capacity estimation, channels with memory, data-driven, neural polar decoders, polar codes.

## I. INTRODUCTION

Channel capacity is a fundamental quantity describing the highest rate of reliable communication over a noisy channel when the transmission latency is not limited. However, knowing the channel capacity does not provide a practical coding scheme that performs well within the block lengths commonly used in contemporary communication systems. Evidently, capacity estimation and coding techniques, despite being closely related, have diverged over the years into two distinct directions: algebraic tools have been dominant in coding, while probabilistic approaches have been prevalent in capacity estimation.

This paper was presented in part at the International Symposium on Information Theory (ISIT) 2024 [1]. This research was supported in part by the National Science Foundation (NSF) under Grant 2308445 and by the NSF-Israel Binational Science Foundation (BSF) under Grant 3211/23. The views expressed are those of the authors and do not necessarily reflect those of the NSF or BSF. Source code and implementation details are available at: <https://github.com/zivaharoni/neural-polar-decoders>.

In the context of capacity estimation, the literature is abundant with instances addressing this problem. Notable works include the Blahut-Arimoto algorithm and its extensions [2]–[5], as well as algorithms for the estimation of the directed information (DI) [6]–[9], which has been shown to be a unifying measure for the characterization of channel capacity [10]. In recent years, the rise of machine learning algorithms has significantly impacted the field of capacity estimation, providing new research directions and enhancing the capabilities of traditional algorithms. New neural network (NN)-based estimators for channel capacity have emerged, such as those in [11]–[15]. Even though there are many instances of capacity estimation techniques, none of which, except for special cases, provide practical coding schemes.

In this work, we aim to address this gap by devising a capacity estimation algorithm that also provides a practical coding scheme. The setting considered here assumes the absence of a channel model, treating the channel as a black-box that produces samples of channel outputs for input samples chosen by the designer. Our objectives under this setting are threefold: 1) to devise a model capable of estimating the mutual information (MI) between the channel inputs and outputs from samples, 2) to optimize the input distribution with respect to the MI, and 3) to use the optimized model to construct practical codes.

In order to achieve all three objectives, we employ polar codes [16]. Polar codes constitute the first deterministic construction of capacity-achieving codes for binary memoryless symmetric (BMS) channels with an efficient successive cancellation (SC) decoder. Enhancing polar codes with successive cancellation list (SCL) decoding and the addition of cyclic redundancy check (CRC) outer codes [17] has dramatically improved their performance for moderate block lengths, leading to their adoption in the 5G standard [18]. Recently, the authors proposed to use NNs in polar codes, denoted by neural polar decoders (NPDs), in order to address cases where a channel model is not known and possibly has memory [19]. In this work, we take one step forward and use NPDs to optimize the input distribution of the code and adapt it to list decoding.

The methodology proposed herein employs NPDs [19] and uses them as a fundamental ingredient. The methodology is divided into two phases: a training phase, in which samples are used to simultaneously estimate an NPD and optimize the input distribution, and an inference phase, in which the optimized model is fixed and used to construct the code.

The training phase is composed of an alternated maximization procedure, in which two core steps are repeated interchangeably. The first step is the estimation step, in which

the parameters of the NPDs are updated to estimate the MI incurred by a fixed input distribution. The second step is the improvement step, in which the NPDs's parameters are fixed, and are used to optimize the parameters of the input distribution. This procedure continues until the convergence of the algorithm.

In the inference phase, the parameters of the input distribution and the NPD are fixed and used to construct a polar code. To accommodate with the optimized input distribution, that is generally not uniform and independent and identically distributed (i.i.d.), we use the Honda-Yamamoto (HY) scheme for the code construction, encoder and decoder [20]. Specifically, the construction of the code is performed by a Monte Carlo (MC) evaluation of the synthetic channels, and the encoder and decoder are implemented as described in [20]. To enhance the code performance, we also incorporated list decoding [17] with the NPDs, which had a pivotal impact in our experiments.

In the experiments, we illustrate the performance of our method on memoryless channels and finite state channels (FSCs). Specifically, we showcase the estimated MI of the optimized input distribution and the incurred bit error rate (BER). For comparison, we compare our results to known lower and upper bounds on capacity from the literature and show that the optimized MI converges to the lower bound from the literature [21]. We also demonstrate the increase in MI of the optimized input distribution in comparison to an i.i.d. input distribution. To complete the experiments, we compare the BERs incurred by the optimized input distribution and an i.i.d. input distribution, showcasing an improvement of one order of magnitude for block lengths of 1024.

### A. Contributions

This paper presents the following contributions:

- 1) Simultaneous input distribution optimization and code construction: We introduce a novel method that simultaneously maximizes input distributions and constructs practical codes through the application of NPDs.
- 2) Neural polar decoders with SCL decoding: We demonstrate that NPDs can be effectively utilized with SCL decoding. This integration shows promising performance improvements, enhancing the practical utility of NPDs.
- 3) Experimental validation and scalability: We validate our approach through extensive experiments, showing the quality of our method in optimizing MI and reducing BERs in comparison to uniform and i.i.d. input distributions. Our results demonstrate its effectiveness for block lengths up to 1024, suggesting that our method is scalable and potentially applicable to real-world communication systems.

### B. Organization

The remainder of this paper is organized as follows. Section II provides the notations and necessary preliminaries. Section III provides a comprehensive description of NPDs, including

their structure and decoding process. It also introduces the key advancements made in this work, such as a fast estimation algorithm for NPDs parameters and their integration with SCL decoding. Section IV addresses the problem of optimizing input distributions to maximize the MI. Section V presents experimental results on capacity estimation and code design for various communication channels, including the Ising and Trapdoor channels. Finally, Section VI concludes the paper, summarizing the contributions and suggesting directions for future research.

## II. NOTATIONS AND PRELIMINARIES

Throughout this paper, we denote by  $(\Omega, \mathcal{B}, \mathbb{P})$  the underlying probability space upon which all random variables are defined. Here,  $\Omega$  is the set of all two-sided infinite sequences of real numbers, represented by  $\omega = (\dots, \omega_{-1}, \omega_0, \omega_1, \dots)$ , with each  $\omega_i \in \mathbb{R}$  for every integer  $i$ . The symbol  $\mathcal{B}$  denotes the corresponding Borel  $\sigma$ -algebra, ensuring that events involving these sequences are well-defined and measurable. The probability measure, denoted by  $\mathbb{P}$ , is chosen to be the Lebesgue measure, which facilitates the assignment of probabilities to events within  $\mathcal{B}$ . Lastly,  $\mathbb{E}$  denotes the expectation operator, used to calculate the expected value of random variables defined over this probability space.

Random variables (RVs) are denoted by capital letters and their realizations by lower-case letters, e.g.,  $X$  and  $x$ , respectively. Calligraphic letters denote sets, e.g.,  $\mathcal{X}$ . We use the notation  $X_i^j$  to denote the RV  $(X_i, X_{i+1}, \dots, X_j)$ , and  $x_i^j$  to denote its realization for  $i < j$ . If  $i = 1$ , we may omit the index  $i$  to simplify notation, i.e., we use the shorthand  $X^j$ . The probability  $\Pr[X = x]$  is denoted by  $P_X(x)$ . Stochastic processes are denoted by blackboard bold letters, e.g.,  $\mathbb{X} := (X_i)_{i \in \mathbb{N}}$ . An  $n$ -coordinate projection of  $\mathbb{P}$  is denoted by  $P_{X^n Y^n} := \mathbb{P}|_{\sigma(X^n, Y^n)}$ , where  $\sigma(X^n, Y^n)$  is the  $\sigma$ -algebra generated by  $(X^n, Y^n)$ . For a given decomposition of  $P_{X^n, Y^n}$  into  $P_{X^n}$  and  $P_{Y^n|X^n}$ , we denote by  $P_{X^n} \otimes P_{Y^n|X^n}$  the joint distribution obtained by  $P_{X^n}(x^n)P_{Y^n|X^n}(y^n|x^n)$  for every  $x^n, y^n \in \mathcal{X}^n \times \mathcal{Y}^n$ .

The MI between two RVs  $X, Y$  is denoted by  $I(X; Y)$ . For two distributions  $P, Q$ , the cross entropy (CE) is denoted by  $h_{\text{CE}}(P, Q)$ , the entropy is denoted by  $H(P)$  and the Kullback Leibler (KL) divergence is denoted by  $D_{\text{KL}}(P||Q)$ . The notation  $P \ll Q$  indicates that  $P$  is absolutely continuous with respect to (w.r.t.)  $Q$ . We denote by  $[K : N]$  the set of integers  $\{K, \dots, N\}$  for  $K < N$ .

The tuple  $(W_{Y|X}, \mathcal{X}, \mathcal{Y})$  defines a memoryless channel with input alphabet  $\mathcal{X}$ , output alphabet  $\mathcal{Y}$  and a transition kernel  $W_{Y|X}$ . Throughout the paper we assume that  $\mathcal{X} = \mathbb{F}_2$ , where  $\mathbb{F}_2$  is the Galois field with two elements,  $\{0, 1\}$ . For a memoryless channel, we denote its input distribution by  $P_X = P_{X_i}$  for all  $i \in \mathbb{Z}$ . The tuple  $(W_{Y||X}, \mathcal{X}, \mathcal{Y})$  defines a time-invariant channel with memory, where  $W_{Y||X} = \left\{ W_{Y_0|Y_{-i+1}^{-1}, X_{-i+1}^0} \right\}_{i \in \mathbb{N}}$ , and  $X_{-i}^0 = (X_{-i}, X_{-i+1}, \dots, X_{-1}, X_0)$ . The term  $W_{Y^N||X^N} = \prod_{i=1}^N W_{Y_0|Y_{-i+1}^{-1}, X_{-i+1}^0}$  denotes the probability of observing

$Y^N$  causally conditioned on  $X^N$  [22]. The symmetric capacity of a channel is denoted by  $I(W)$ . We denote by  $\mathcal{D}_{M,N} = \{x_{j,i}, y_{j,i}\}_{j \in [M], i \in [N]} \sim P_{X^{MN}} \otimes W_{Y^{MN} | X^{MN}}$  a finite sample of input-output pairs of  $M$  consecutive blocks of  $N$  symbols, where  $x_{j,i}, y_{j,i}$  denotes the  $i$ -th input and output of the  $j$ -th block. The notation  $x_{j,1}^N$  denotes the collection  $\{x_{j,i}\}_{i=1}^N$ . The term  $\mathcal{D}_{MN} = \{x_i, y_i\}_{i \in [MN]}$  denotes the same sample as  $\mathcal{D}_{M,N}$  after its concatenation into one long sequence of inputs and outputs pairs.

### A. Polar Codes for Symmetric Channels

Let  $G_N = B_N F^{\otimes n}$  represent the generator matrix for a block length of  $N = 2^n$ , where  $n \in \mathbb{N}$ , defining what is known as Arikan's polar transform. The matrix  $B_N$  is the permutation matrix associated with the bit-reversal permutation. It is defined by the recursive relation  $B_N = R_N(I_2 \otimes B_{\frac{N}{2}})$  starting from  $B_2 = I_2$ . The term  $I_N$  denotes the identity matrix of size  $N$  and  $R_N$  denotes a permutation matrix called reverse-shuffle [16]. The matrix  $G_N$  satisfies  $G_N G_N = I_N$ . The term  $A \otimes B$  denotes the Kronecker product of  $A$  and  $B$ . The term  $A^{\otimes N} := A \otimes A \otimes \dots \otimes A$  denotes an application of the  $\otimes$  operator  $N$  times.

We define a polar code by the tuple  $(\mathcal{X}, \mathcal{Y}, W, E, F, G, H)$  that contains the channel  $W$ , the channel embedding  $E$  and the core components of the SC decoder,  $F, G, H$ . We define the synthesized channels by the tuple  $(W_N^{(i)}, \mathcal{X}, \mathcal{X}^{i-1} \times \mathcal{Y}^N)$  for all  $i \in [N]$ . The term  $E : \mathcal{Y} \rightarrow \mathcal{E}$  denotes the channel embedding, where  $\mathcal{E} \subset \mathbb{R}^d$ . It is also referred in the literature by the term channel statistics, but here for our purposes, we alternatively choose to call it the channel embedding. For example, for a memoryless channel  $W := W_{Y|X}$ , a valid choice of  $E$ , as used in the remainder of this paper, is given by the following:

$$E(y) = \log \frac{W(y|1)}{W(y|0)} + \log \frac{P_X(1)}{P_X(0)}, \quad (1)$$

where the second term in the right-hand-side (RHS) cancels out in the case where  $P_X$  is uniform.

The functions  $F : \mathcal{E} \times \mathcal{E} \rightarrow \mathcal{E}$ ,  $G : \mathcal{E} \times \mathcal{E} \times \mathcal{X} \rightarrow \mathcal{E}$  denote the check-node and bit-node operations, respectively. We denote by  $H : \mathcal{E} \rightarrow \mathbb{R}$  a mapping of the embedding into an log likelihood ratio (LLR) value, i.e. a soft-decision. For memoryless channels and with the selection of  $E$  as defined in Equation (1), the functions  $F$ ,  $G$ , and  $H$  are specified as follows:

$$\begin{aligned} F(e_1, e_2) &= -2 \tanh^{-1} \left( \tanh \frac{e_1}{2} \tanh \frac{e_2}{2} \right), \\ G(e_1, e_2, u) &= e_2 + (-1)^u e_1, \\ H(e_1) &= e_1, \end{aligned} \quad (2)$$

where  $e_1, e_2 \in \mathbb{R}, u \in \mathcal{X}$ . For this choice, the hard decision rule  $h : [0, 1] \rightarrow \mathcal{X}$  is the sign function  $h(l) = \mathbb{I}_{l > 0.0}$ , where  $\mathbb{I}$  is the indicator function. Applying SC decoding on the channel outputs yields an estimate of the transmitted bits and their

corresponding posterior distribution [16]. Specifically, after observing  $y_1^N$ , SC decoding performs the map

$$(y_1^N, f_1^N) \mapsto \left\{ \hat{u}_i, L_{U_i | U_1^{i-1}, Y_1^N}(\hat{u}_1^{i-1}, y_1^N) \right\}_{i \in [N]},$$

where

$$L_{U_i | U_1^{i-1}, Y_1^N}(u_1^{i-1}, y_1^N) = \log \frac{P_{U_i | U_1^{i-1}, Y_1^N}(1 | u_1^{i-1}, y_1^N)}{P_{U_i | U_1^{i-1}, Y_1^N}(0 | u_1^{i-1}, y_1^N)} \quad (3)$$

is the LLR function. The term  $f_1^N$  represents the common information between the encoder and the decoder by setting

$$f_i = \begin{cases} u_i & i \in \mathcal{A}^c \\ 0.5 & i \in \mathcal{A} \end{cases},$$

where the value 0.5 is chosen arbitrarily to indicate that the bit needs to be decoded, the set  $\mathcal{A} \subseteq [N]$  is the information set and  $\mathcal{A}^c = [N] \setminus \mathcal{A}$  is the frozen set. For more details on SC decoding, the reader may refer to [16, Section VIII].

### B. SC List Decoding

To enhance the error correction performance of polar codes, especially with codes of moderate lengths, the SCL decoding algorithm was introduced in [17]. The fundamental concept behind list decoding lies in leveraging the structured nature of the polar transformation. Instead of relying solely on a single SC decoder, the SCL decoder concurrently decodes multiple codeword candidates. This is achieved by applying multiple SC decoders over the same channel's outputs, with the number of these decoders denoted as the list size  $L$ .

The SCL decoder generates a list of potential codewords, each ranked by its likelihood of being the transmitted message. To achieve this, the SCL algorithm estimates each bit's value (0 or 1) while considering both possibilities. At each estimation step, the number of codeword candidates (also referred to as paths) doubles. To manage the algorithm's complexity, it employs a memory-saving strategy by retaining only a limited set of  $L$  codeword candidates at any given time. To decide which paths to retain, a path metric is assigned to each path, determining its likelihood. After the generation of  $L$  paths, the SCL decoder chooses the codeword with the best path metric.

### C. Neural Networks

The class of shallow NNs, i.e. NNs with one hidden layer and with fixed input and output dimensions, is defined as follows [23].

**Definition 1** (NN function class). For the ReLU activation function  $\sigma_{\mathbb{R}}(x) = \max(x, 0)$  and  $d_i, d_o \in \mathbb{N}$ , define the class of neural networks with  $k \in \mathbb{N}$  neurons as:

$$\mathcal{G}_{\text{NN}}^{(d_i, k, d_o)} := \left\{ g : \mathbb{R}^{d_i} \rightarrow \mathbb{R}^{d_o} : g(x) = \sum_{j=1}^k \beta_j \sigma_{\mathbb{R}}(W_j x + b_j), x \in \mathbb{R}^{d_i} \right\}, \quad (4)$$

where  $\sigma_R$  acts component-wise,  $\beta_j \in \mathbb{R}$ ,  $W_j \in \mathbb{R}^{d_o \times d_i}$  and  $b_j \in \mathbb{R}^{d_o}$  are the parameters of  $g \in \mathcal{G}_{\text{NN}}^{(d_i, k, d_o)}$ . Then, the class of NNs with input and output dimensions  $(d_i, d_o)$  is given by

$$\mathcal{G}_{\text{NN}}^{(d_i, d_o)} := \bigcup_{k \in \mathbb{N}} \mathcal{G}_{\text{NN}}^{(d_i, k, d_o)}, \quad (5)$$

and the class of NNs is given by  $\mathcal{G}_{\text{NN}} := \bigcup_{d_i, d_o \in \mathbb{N}} \mathcal{G}_{\text{NN}}^{(d_i, d_o)}$ .

#### D. Communication Channels

The channels selected in this study are chosen to validate our methodology through the experiments detailed in Section V. Specifically, we focus on the additive white Gaussian noise (AWGN), Ising, and Trapdoor channels. These channels serve as examples of both memoryless channels and FSCs. The primary rationale behind selecting these channels is to assess the performance of the NPD against established theoretical benchmarks. For memoryless channels, we employ the SC decoder [16] as a theoretical benchmark, while for FSCs, we use the successive cancellation trellis (SCT) decoder as described in [24]. The definitions of the channels are provided below.

The AWGN channel is defined by the following model

$$Y_i = X_i + N_i$$

where  $N_i \stackrel{i.i.d.}{\sim} \mathcal{N}(0, \sigma^2)$  and  $X_i$  is the channel input subject to the average power constraint  $E[X_i^2] \leq P$ . The Ising channel [25] is an instance of FSCs and is defined by

$$Y_i = \begin{cases} X_i & \text{with probability } 0.5 \\ X_{i-1} & \text{with probability } 0.5. \end{cases}$$

The Trapdoor channel, introduced by Blackwell as a "two-state simple channel" [26]. It is defined by:

$$Y_i = \begin{cases} X_i & \text{with probability } 0.5 \\ S_{i-1} & \text{with probability } 0.5, \end{cases}$$

and the channel state evolves according to the following deterministic rule  $S_i = S_{i-1} + X_i + Y_i \pmod{2}$ .

### III. NEURAL POLAR DECODERS

The purpose of this section is twofold. First, it aims to provide the necessary background on NPDs, as introduced in the authors' previous work [19]. Second, it introduces two important advancements over the work presented in [19]. These advancements include a fast estimation algorithm for the NPD's parameters and its integration with list decoding [17]. Specifically, Sections III-A, III-B, and III-E contain material from the authors' previous work, whereas Sections III-C and III-D present the new advancements.

#### A. Structure of the NPD

Let  $X^N, Y^N$  be the channel inputs and outputs, respectively, and define  $U^N = X^N G_N$ . An NPD operates by decoding  $Y^N$  into  $\hat{U}^N$  via a SC procedure. The SC procedure systematically decodes the information bits sequentially, utilizing the four core functions: embedding function  $E$ , check-node function  $F$ , bit-node function  $G$ , and embedding-to-LLR function  $H$ , which are repeatedly applied throughout the decoding process. In an NPD, these four functions are approximated by NNs. The subsequent definitions explain the NPD by describing its two primary blocks

**Definition 2** (Channel Embedding). Let  $E_{\theta_E} : \mathcal{Y} \rightarrow \mathbb{R}^d$  be the NN that embeds the channel outputs into the embedding space of the NPD, where  $d \in \mathbb{N}$  is the dimension of the embedding space. For  $\mathcal{Y} \subset \mathbb{R}$ , we define  $E_{\theta_E} \in \mathcal{G}_{\text{NN}}^{(1, k, d)}$  to be the embedding NN, where  $k \in \mathbb{N}$  is the number of hidden units.

**Definition 3** (Neural Polar Decoder). Let  $F_{\theta_F}, G_{\theta_G}, H_{\theta_H}$  be the NNs components of the NPD. The NPD's NNs are defined by

- $F_{\theta_F} \in \mathcal{G}_{\text{NN}}^{(2d, k, d)}$  is the check-node NN,
- $G_{\theta_G} \in \mathcal{G}_{\text{NN}}^{(2d+1, k, d)}$  is the bit-node NN,
- $H_{\theta_H} \in \mathcal{G}_{\text{NN}}^{(d, k, 1)}$  is the embedding-to-LLR NN,

where  $d \in \mathbb{N}$  is the dimension of the embedding space and  $k \in \mathbb{N}$  is the number of hidden units.

In the rest of the paper, we adopt the notation  $\theta = \{\theta_E, \theta_F, \theta_G, \theta_H\}$  for simplicity. The distinction between Definitions 2 and 3 arises because the same NPD may be used for two different channel embeddings. This is illustrated in Section IV, where we use the same NPD to implement the HY scheme [20].

#### B. SC Decoding with the NPD

The NPD's SC decoder is defined by applying the recursive formulas of SC decoding [16] with  $E_\theta, F_\theta, G_\theta$ , and  $H_\theta$  instead of  $E, F, G, H$ , as given in Equations (1), (2). Specifically, upon observing the channel outputs, the function  $E_\theta$  maps each channel output  $Y_i$  into its embedding representation  $e_{0,i} \in \mathbb{R}^d$ , acting as the belief of  $X_i$  given  $Y_i$ . For example,  $\mathbf{e}_0 = (e_{0,i})_{i=1}^N \in \mathbb{R}^{N \times d}$  represents the belief of  $\mathbf{v}_0 := X^N$ . Next, the NPD uses  $\mathbf{e}_0$  as its input to decode  $U^N$  sequentially by utilizing  $F_\theta, G_\theta$ , and  $H_\theta$ . Accordingly, for any  $j \in [1 : n]$  and  $i \in [1 : N]$ , the recursive formulas are given by

$$e_{j+1, 2i-1} = F_\theta(e_{j,i}, e_{j,i+2^j}), \quad (6)$$

$$e_{j+1, 2i} = G_\theta(e_{j,i}, e_{j,i+2^j}, u_{j+1, 2i-1}). \quad (7)$$

The last function,  $H_\theta$ , converts an embedding  $e_{j,i}$  into an LLR value associated with  $v_{j,i}$ , as defined by

$$l_{j,i} = H_\theta(e_{j,i}), \quad (8)$$

where  $l_{j,i}$  is the estimate of the LLR of  $v_{j,i}$ . The LLRs  $l_{j,i}$  are used to make decisions on the bits  $v_{j,i}$  by applying the hard-

decision function. The outputs of the SC decoder are denoted by  $L_{U_i|U^{i-1}, Y^N}^\theta(\hat{u}^{i-1}, y^N)$  for  $i \in [N]$ .

The computational complexity of SC decoding with the NPD is given next, as shown in [19].

**Theorem 1** (Computational Complexity of the NPD). *Let  $E_\theta \in \mathcal{G}_{\text{NN}}^{(1,k,d)}$ ,  $F_\theta \in \mathcal{G}_{\text{NN}}^{(2d,k,d)}$ ,  $G_\theta \in \mathcal{G}_{\text{NN}}^{(2d+1,k,d)}$  and  $H_\theta \in \mathcal{G}_{\text{NN}}^{(d,k,1)}$ . Then, the computational complexity of SC decoding with the NPD is  $O(kdN \log N)$ .*

The main purpose of Theorem 1 is to facilitate a comparison between the NPD and SCT decoder. Note that the computational complexity of the SCT decoder scales with the memory size of the channel as  $O(|\mathcal{S}|^3 N \log N)$  [24]. This highlights a key advantage of the NPD, as its computational complexity depends on the parameterization of the NPD and not on the channel's state size.

### C. SC List Decoding with the NPD

We point out that list decoding [17] can be easily integrated with the NPD. Recall that the NPD decoder uses the same structure as the SC decoder and the SCT decoder, with the only distinction being the replacement of elementary operations with NNs. Accordingly, we can seamlessly incorporate list decoding into the NPD decoder. Specifically, since the NPD decoding algorithm can estimate the LLRs at the decision points, we can leverage them to compute the path-metric and follow the same SCL decoding procedure. The following theorem shows the computational complexity of the NPD list decoder for the case where  $E_\theta, F_\theta, G_\theta, H_\theta$  are NNs with  $k$  hidden units and the embedding space has  $d$  dimensions.

**Theorem 2.** *Let  $E_\theta \in \mathcal{G}_{\text{NN}}^{(1,k,d)}$ ,  $F_\theta \in \mathcal{G}_{\text{NN}}^{(2d,k,d)}$ ,  $G_\theta \in \mathcal{G}_{\text{NN}}^{(2d+1,k,d)}$  and  $H_\theta \in \mathcal{G}_{\text{NN}}^{(d,k,1)}$ . Then, the computational complexity of SCL decoding with the NPD and list size  $L$  is  $O(LkdN \log N)$ .*

### D. Estimating the NPD's parameters

The parameters of the NPD are determined in a training phase. The goal of the training phase is to tune  $\theta$  such that its outputs would match the true LLRs  $L_{U_i|U^{i-1}, Y^N}(y^N, u^{i-1})$ ,  $i \in [1 : N]$ , as defined in (3). For memoryless channels, the NPD is trained to approximate the "vanilla" SC decoder [16]; for FSCs, the NPD is trained to approximate the SCT decoder [24]. The training procedure of the NPD involves an iterative process. During each iteration, samples of channel input-output pairs are used to compute the gradient for updating  $\theta$  via stochastic gradient descent (SGD) optimization. The training algorithm is given in Algorithm 2, and it is described hereafter.

Let  $\mathcal{D}_{M,N} \sim P_{X^{MN}} \otimes W_{Y^{MN}||X^{MN}}$  be a finite sample of input-output pairs consisting of  $M$  consecutive blocks of  $N$  symbols. At each iteration of the algorithm, a block  $(x^N, y^N) \sim \mathcal{D}_{M,N}$  is drawn uniformly and used to compute  $\mathcal{L}(x^N, y^N; \theta)$ , the loss for estimating the NPD's parameters,

as shown in [19]. After computing the loss, the gradient  $\nabla_\theta \mathcal{L}(x^N, y^N; \theta)$  is computed to update the parameters of the NPD using SGD. This iterative scheme continues until the algorithm converges, either after a predetermined number of steps  $N_{\text{iter}}$ , or when  $\mathcal{L}(x^N, y^N; \theta)$  stops decreasing. The overall algorithm is outlined in Algorithm 2.

In [19], the loss of the NPD is computed via the recursive formulas of the SC decoding algorithm. Here, we enhance the gradient computation by calculating the loss stage-by-stage rather than through recursion. This improvement reduces the number of computational steps of the loss computation from  $N \log(N)$  to  $\log(N)$ . Although the computational method has been modified, the guarantees of the algorithm remain intact because the underlying mathematical framework is preserved. The details of the loss computation are described next.

1) *Loss Computation:* Given  $x^N$  and  $y^N$ , the loss of the NPD is computed as follows. First, the embeddings of  $\mathbf{v}_0 = x^N$  are computed as  $\mathbf{e}_0 = \mathbf{E}_\theta(y^N)$ , where  $\mathbf{E}_\theta$  denotes the component-wise application of  $E_\theta$  on each element of  $y^N$ . Similarly, the LLRs are computed as  $\mathbf{l}_0 = \mathbf{H}_\theta(\mathbf{e}_0)$ . The loss of the bits at stage 0 is then computed by:

$$\begin{aligned} \mathcal{L}_0(\mathbf{v}_0, \mathbf{e}_0; \theta) = & \\ & - \frac{1}{N} \sum_{i=1}^N v_{0,i} \log \sigma(l_{0,i}) + \bar{v}_{0,i} \log \overline{\sigma(l_{0,i})}, \end{aligned} \quad (9)$$

where  $\bar{x} = 1 - x$ ,  $\sigma(x) = \frac{1}{1+e^{-x}}$  is the logistic function and  $P_{U_i|U^{i-1}, Y^N}(1|u^{i-1}, y^N) = \sigma(L_{U_i|U^{i-1}, Y^N}(u^{i-1}, y^N))$ .

At stage 1, the loss is computed in the following manner. First,  $\mathbf{v}_1$  is computed by

$$\mathbf{v}_1 = [\mathbf{v}_0^o \oplus \mathbf{v}_0^e \mid \mathbf{v}_0^e], \quad (10)$$

where  $\mathbf{v}_0^o, \mathbf{v}_0^e \in \mathbb{F}_2^{\frac{N}{2}}$  contain the odd and even elements of  $\mathbf{v}_0$ , respectively. Next,  $\mathbf{e}_1$  is computed by:

$$\mathbf{e}_1 = [\mathbf{F}_\theta(\mathbf{e}_0^o, \mathbf{e}_0^e) \mid \mathbf{G}_\theta(\mathbf{e}_0^o, \mathbf{e}_0^e, \mathbf{v}_0^o \oplus \mathbf{v}_0^e)], \quad (11)$$

where  $\mathbf{F}_\theta(\mathbf{e}_0^o, \mathbf{e}_0^e)$ ,  $\mathbf{G}_\theta(\mathbf{e}_0^o, \mathbf{e}_0^e, \mathbf{v}_0^o \oplus \mathbf{v}_0^e) \in \mathbb{R}^{\frac{N}{2} \times d}$ , the operator  $[\cdot \mid \cdot]$  denotes the concatenation of two matrices along the first dimension, and  $\mathbf{e}_1 \in \mathbb{R}^{N \times d}$ . The loss of stage 1 is then computed by first computing:

$$\mathbf{l}_1 = \mathbf{H}_\theta(\mathbf{e}_1), \quad (12)$$

and then computing  $\mathcal{L}_1(\mathbf{v}_1, \mathbf{e}_1; \theta)$ , as done in stage 0.

At stages  $j \in [2 : n]$ , the same computations as in stage 1 are followed, but they are performed within sub-blocks independently. Given  $\mathbf{e}_{j-1}$  and  $\mathbf{v}_{j-1}$ , we first split them into the collections:

$$\begin{aligned} \mathbf{v}^{(j-1)} &= \{\mathbf{v}_{j-1,k}\}_{k=0}^{2^{j-1}-1} \\ \mathbf{e}^{(j-1)} &= \{\mathbf{e}_{j-1,k}\}_{k=0}^{2^{j-1}-1}, \end{aligned} \quad (13)$$

where

$$\begin{aligned} \mathbf{v}_{j-1,k} &= \{v_{j-1,l}\}_{l=1+k2^{n-j+1}}^{(k+1)2^{n-j+1}} \\ \mathbf{e}_{j-1,k} &= \{e_{j-1,l}\}_{l=1+k2^{n-j+1}}^{(k+1)2^{n-j+1}}, \end{aligned}$$

**Algorithm 1** Loss Computation for Neural Polar Decoders

**Input:**  
 $x^N, y^N$   $\triangleright$  Channel input-output pairs  
 $E_\theta, F_\theta, G_\theta, H_\theta$   $\triangleright$  NPD model  
**Output:**  
 $\mathcal{L}(x^N, y^N; \theta)$   $\triangleright$  computed loss

**Stage 0:**

$\mathbf{v}_0 \leftarrow x^N$   
 $\mathbf{e}_0 \leftarrow \mathbf{E}_\theta(y^N)$   
 $\mathbf{l}_0 \leftarrow \mathbf{H}_\theta(\mathbf{e}_0)$   
 $\mathcal{L}_0(\mathbf{v}_0, \mathbf{e}_0; \theta) = -\frac{1}{N} \sum_{i=1}^N v_{0,i} \log \sigma(l_{0,i}) + \bar{v}_{0,i} \log \overline{\sigma(l_{0,i})}$   
 $\triangleright$  loss of stage 0

**Stage 1:**

$\mathbf{v}_1 \leftarrow [\mathbf{v}_0^o \oplus \mathbf{v}_0^e \mid \mathbf{v}_0^e]$   
 $\mathbf{e}_1 \leftarrow [\mathbf{F}_\theta(\mathbf{e}_0^o, \mathbf{e}_0^e) \mid \mathbf{G}_\theta(\mathbf{e}_0^o, \mathbf{e}_0^e, \mathbf{v}_0^o \oplus \mathbf{v}_0^e)]$   
 $\mathbf{l}_1 \leftarrow \mathbf{H}_\theta(\mathbf{e}_1)$   
 $\mathcal{L}_1(\mathbf{v}_1, \mathbf{e}_1; \theta) = -\frac{1}{N} \sum_{i=1}^N v_{1,i} \log \sigma(l_{1,i}) + \bar{v}_{1,i} \log \overline{\sigma(l_{1,i})}$   
 $\triangleright$  loss of stage 1

**Stages 2 to n:**

**for**  $j = 2$  to  $n$  **do**  
 Compute  $\mathbf{v}^{(j-1)}$  and  $\mathbf{e}^{(j-1)}$   $\triangleright$  Equation (13)  
 Initiate  $\mathbf{v}^{(j)} = \emptyset, \mathbf{e}^{(j)} = \emptyset, \mathbf{l}^{(j)} = \emptyset$   
**for each**  $\tilde{\mathbf{v}}_{j-1} \in \mathbf{v}^{(j-1)}$  and  $\tilde{\mathbf{e}}_{j-1} \in \mathbf{e}^{(j-1)}$  **do**  
 Compute  $\tilde{\mathbf{v}}_j, \tilde{\mathbf{e}}_j$  and  $\tilde{\mathbf{l}}_j$   $\triangleright$  Equation (10)–(12)  
 $\mathbf{v}^{(j)} \leftarrow \mathbf{v}^{(j)} \cup \tilde{\mathbf{v}}_j, \mathbf{e}^{(j)} \leftarrow \mathbf{e}^{(j)} \cup \tilde{\mathbf{e}}_j, \mathbf{l}^{(j)} \leftarrow \mathbf{l}^{(j)} \cup \tilde{\mathbf{l}}_j$   
**end for**  
 Concatenate  $\mathbf{v}^{(j)}, \mathbf{e}^{(j)}, \mathbf{l}^{(j)}$  into  $\mathbf{e}_j, \mathbf{v}_j, \mathbf{l}_j$   
 $\mathcal{L}_j(\mathbf{v}_j, \mathbf{e}_j; \theta) = -\frac{1}{N} \sum_{i=1}^N v_{j,i} \log \sigma(l_{j,i}) + \bar{v}_{j,i} \log \overline{\sigma(l_{j,i})}$   
 $\triangleright$  loss of stage  $j$   
**end for**  
**return**  $\mathcal{L}(x^N, y^N; \theta) \leftarrow \frac{1}{n+1} \sum_{j=0}^n \mathcal{L}_j(\mathbf{v}_j, \mathbf{e}_j; \theta)$

with  $\mathbf{v}_{j-1,k} \in \mathbb{F}_2^{\frac{N}{2^{j-1}} \times 1}$  and  $\mathbf{e}_{j-1,k} \in \mathbb{R}^{\frac{N}{2^{j-1}} \times d}$ . For every  $\mathbf{v}_{j-1,k}$  and  $\mathbf{e}_{j-1,k}$ , we repeat the computations in Equations (10)–(11) to produce  $\mathbf{v}'_{j-1,k}$  and  $\mathbf{e}'_{j-1,k}$ , which are then concatenated into  $\mathbf{e}_j, \mathbf{v}_j$ . Next,  $\mathbf{e}_j, \mathbf{v}_j$  are used to compute  $\mathcal{L}_j(\mathbf{v}_j, \mathbf{e}_j; \theta)$  and are passed to the next stage. The overall loss is computed by

$$\mathcal{L}(x^n, y^n; \theta) = \frac{1}{n+1} \sum_{j=0}^n \mathcal{L}_j(\mathbf{v}_j, \mathbf{e}_j; \theta), \quad (14)$$

and the corresponding gradient is given by  $\nabla_\theta \mathcal{L}(x^n, y^n; \theta)$ . The loss computation is summarized in Algorithm 1.

**E. Consistency of the NPD Estimation**

In [19], Algorithm 2 was shown to be consistent. That is, as  $M$  approaches infinity, the optimized NPD recovers the conditional entropies of the effective channels. The consistency of the NPD [19, Theorem 4] is given herein.

**Algorithm 2** Data-driven NPD Estimation

**input:** Dataset  $\mathcal{D}_{M,N}$ , #of iterations  $N_{\text{iters}}$ , learning rate  $\gamma$   
**output:** Optimized  $\theta^*$

Initiate the weights of  $E_\theta, F_\theta, G_\theta, H_\theta$   
**for**  $N_{\text{iters}}$  iterations **do**  
 Sample  $x^N, y^N \sim \mathcal{D}_{M,N}^\psi$   
 Compute  $\mathcal{L}(x^N, y^N; \theta)$   $\triangleright$  Equation (14)  
 Update  $\theta := \theta - \gamma \nabla_\theta \mathcal{L}(x^N, y^N; \theta)$   
**end for**  
**return**  $\theta^*$

**Theorem 3.** Let  $\mathbb{X}, \mathbb{Y}$  be the inputs and outputs of an indecomposable FSC. Let  $\mathcal{D}_{M,N} \sim P_{X^{MN}} \otimes W_{Y^{MN} \| X^{MN}}$ , where  $N = 2^n$ ,  $M, n \in \mathbb{N}$ . Let  $u_{j,i} = (x_{j,1}^N G_N)_i$ . Then, for every  $\varepsilon > 0$  there exists  $p \in \mathbb{N}$ , compact  $\Theta \in \mathbb{R}^p$  and  $m \in \mathbb{N}$  such that for  $M > m$  and  $i \in [N]$ ,  $\mathbb{P} - a.s.$

$$|\mathbf{H}_\Theta^M(U_i | U^{i-1}, Y^N) - \mathbf{H}(U_i | U^{i-1}, Y^N)| < \varepsilon, \quad (15)$$

where

$$\mathbf{H}_\Theta^M(U_i | U^{i-1}, Y^N) = \min_{\theta \in \Theta} \left\{ \frac{1}{M} \sum_{j=1}^M -\log \sigma(l_\theta(y^N, u^i)) \right\}. \quad (16)$$

**IV. INPUT DISTRIBUTION OPTIMIZATION**

This section addresses the problem of choosing an input distribution  $P_{X^N}^\psi$  that maximizes  $\mathbf{I}(X_\psi^N; Y^N)$ . From this section onwards, the subscript  $\psi$  designates the dependence of the MI on the specific input distribution parameterized by  $\psi$ . The process of determining an input distribution that maximizes  $\mathbf{I}(X_\psi^N; Y^N)$  is composed of two main steps. In the first step, the input distribution is fixed. For a fixed  $\psi$ , Algorithm 2 is employed to estimate  $\mathbf{I}(X_\psi^N; Y^N)$ . In the second step, the parameters of the NPD are fixed. For a fixed NPD, the gradient of the input distribution  $\psi$  is computed. Together, these two steps complement each other and are applied interchangeably to form an alternated maximization procedure. This completes the overview of the rate optimization scheme that is detailed herein. Section IV-A describes the parametric model we used for  $P_{X^N}^\psi$ . Section IV-B illustrates the estimation step. Section IV-C describes the optimization step. Section IV-D concludes with the overall algorithm.

**A. Parametric model of the input distribution**

The input distribution is parameterized using a long short-term memory (LSTM) model [27], as detailed herein. Let  $\psi = \{\psi_1, \psi_2\}$  be the parameters of the following model:

$$\begin{aligned} [h_{i+1}, c_{i+1}] &= \text{LSTM}_{\psi_1}(x_i, h_i, c_i) \\ o_i &= W_{\psi_2} h_i + b_{\psi_2}, \end{aligned} \quad (17)$$

where  $\text{LSTM}_{\psi_1}$  acts as a kernel that takes as an input  $x_i \in \mathbb{F}_2$  and current states  $h_i, c_i$ , and outputs its next inner state and

outer state,  $c_{i+1}, h_{i+1} \in \mathbb{R}^k$ , respectively. The initial states  $c_1, h_1 \in \mathbb{R}^k$  are set arbitrarily as zero vectors. A linear transformation is then applied to  $h_i$  using  $W_{\psi_2} \in \mathbb{R}^{1 \times k}$  and  $b_{\psi_2} \in \mathbb{R}$ . In Equation (17), the output  $o_i$  forms the LLR at time  $i$  denoted by  $L_{X_i|X^{i-1}}^\psi(x^{i-1})$ , as it is a function of  $x^{i-1}$  through the states  $c_i$  and  $h_i$ .

Given  $\psi$ , sampling a sequence  $x^N \sim P_{X^N}^\psi$  involves the following steps. Let  $A^N$  be a sequence of i.i.d. RVs with  $A_1 \sim \text{Unif}[0, 1]$ . For every  $i \geq 1$ ,  $x_i$  is sampled according to the following rule:

$$\begin{aligned} o_i &= W_{\psi_2} h_i + b_{\psi_2} \\ x_i &= \mathbb{I}(A_i < \sigma(o_i)) \\ [h_{i+1}, c_{i+1}] &= \text{LSTM}_{\psi_1}(x_i, h_i, c_i). \end{aligned} \quad (18)$$

where  $\sigma(x) = \frac{1}{1+e^{-x}}$  is the logistic function that maps  $L_{X_i|X^{i-1}}^\psi(x^{i-1})$  into  $P_{X_i|X^{i-1}}^\psi(1|x^{i-1})$ . Thus, by using the model in Equation (17) and sampling  $x^N$  by Equation (18), we obtain  $x^N \sim P_{X^N}^\psi$ . The log-likelihood is then evaluated as follows:

$$\log P_{X^N}^\psi(x^N) = \sum_{i=1}^N \left( x_i \log \sigma(o_i) + \bar{x}_i \log \overline{\sigma(o_i)} \right). \quad (19)$$

### B. Step 1: MI Estimation

The estimation step considers a fixed input distribution  $P_{X^N}^\psi$ , and a channel  $W_{Y^N|X^N}$ . These distributions define the joint distribution  $P_{X^N, Y^N}^\psi = P_{X^N}^\psi \otimes W_{Y^N|X^N}$  and the corresponding MI  $\mathfrak{I}(X_\psi^N; Y^N)$ . Since  $U_\psi^N = X_\psi^N G_N$  is bijective, it follows that  $\mathfrak{I}(X_\psi^N; Y^N) = \mathfrak{I}(U_\psi^N; Y^N)$ . By the factorization of the MI as a difference of conditional entropies, we have:

$$\mathfrak{I}(U_\psi^N; Y^N) = \mathfrak{H}(U_\psi^N) - \mathfrak{H}(U_\psi^N | Y^N). \quad (20)$$

Equation (20) suggests that the MI  $\mathfrak{I}(U_\psi^N; Y^N)$  can be estimated by employing the NPD for each term in the RHS of Equation (20). Let an NPD be defined by the NNs  $F_{\theta_F}, G_{\theta_G}, H_{\theta_H}$ , as given in Definition 3. Let  $E_{\theta_{E_1}}, E_{\theta_{E_2}}^\text{co}$  be two channel embeddings, as given in Definition 2. The NN  $E_{\theta_{E_1}}$  embeds the channel outputs to yield  $\mathbf{e}_0 = \mathbf{E}_{\theta_{E_1}}(y^N)$ , while the NN  $E_{\theta_{E_2}}$  produce the embeddings for  $\mathfrak{H}(U^N)$  by embedding constant inputs to yield  $\mathbf{e}_0^\text{co} = \mathbf{E}_{\theta_{E_2}}(\mathbf{0}^N) \in \mathbb{R}^{N \times d}$ . To simplify notation, we define the parameters associated with applying the NPD *after* observing the channel outputs by  $\theta^\text{ch} = \{E_{\theta_{E_1}}, F_{\theta_F}, G_{\theta_G}, H_{\theta_H}\}$ ; the parameter associated with applying the NPD *before* observing the channel outputs by  $\theta^\text{co} = \{E_{\theta_{E_2}}, F_{\theta_F}, G_{\theta_G}, H_{\theta_H}\}$ , and all the parameters by  $\theta = \{\theta^\text{ch}, \theta^\text{co}\}$ .

Application of Algorithm 2 with  $\mathcal{D}_{M,N}^\psi \sim P_{X^{MN}}^\psi \otimes W_{Y^{MN}|X^{MN}}$  as inputs returns  $\theta^\text{ch}$  that enables the estimation of  $\mathfrak{H}(U_\psi^N | Y^N)$ . The estimate is given by

$$\mathfrak{H}_{\theta^\text{ch}}^M(U_\psi^N | Y^N) = \frac{N}{M} \sum_{x^N, y^N \sim \mathcal{D}_{M,N}^\psi} \mathcal{L}(x^N, y^N; \theta^\text{ch}). \quad (21)$$

In the same manner, application of Algorithm 2 with  $\mathcal{D}_{M,N}^\psi \sim P_{X^{MN}}^\psi \otimes \mathbb{I}_{Y=0}^{\otimes MN}$  as inputs returns  $\theta^\text{co}$  that enables the estimation of  $\mathfrak{H}(U_\psi^N)$ . Here,  $\mathbb{I}_{Y=0}$  denotes a constant distribution that assigns the value 0 with probability 1. Accordingly, the estimate of  $\mathfrak{H}(U_\psi^N)$  is given by

$$\mathfrak{H}_{\theta^\text{co}}^M(U_\psi^N) = \frac{N}{M} \sum_{x^N, \mathbf{0}^N \sim \mathcal{D}_{M,N}^\psi} \mathcal{L}(x^N, \mathbf{0}^N; \theta^\text{co}). \quad (22)$$

Together, the parameters  $\theta^\text{ch}$  and  $\theta^\text{co}$  form the parameters for the estimation  $\mathfrak{I}_\psi(U^N; Y^N)$  as given by

$$\begin{aligned} \widehat{\mathfrak{I}}_\Theta^M(U_\psi^N; Y^N) &= \min_{\theta^\text{co} \in \Theta} \frac{N}{M} \sum_{x^N, y^N \sim \mathcal{D}_{M,N}^\psi} \mathcal{L}(x^N, \mathbf{0}^N; \theta^\text{co}) - \\ &\min_{\theta^\text{ch} \in \Theta} \frac{N}{M} \sum_{x^N, y^N \sim \mathcal{D}_{M,N}^\psi} \mathcal{L}(x^N, y^N; \theta^\text{ch}). \end{aligned} \quad (23)$$

We also denote by  $\theta^* = \{\theta^{*\text{co}}, \theta^{*\text{ch}}\}$  the argument achieving the optimum of Equation (23). The following theorem identifies that  $\widehat{\mathfrak{I}}_\Theta^M(U_\psi^N; Y^N)$  is a consistent estimator of  $\mathfrak{I}(U_\psi^N; Y^N)$ .

**Theorem 4.** *Let  $\mathbb{X}, \mathbb{Y}$  be the inputs and outputs of an indecomposable FSC. Let  $\mathcal{D}_{M,N}^\psi \sim P_{X^{MN}}^\psi \otimes W_{Y^{MN}|X^{MN}}$ , where  $N = 2^n$ ,  $M, n \in \mathbb{N}$ . Then, for every  $\varepsilon > 0$  there exists  $p \in \mathbb{N}$ , compact  $\Theta \in \mathbb{R}^p$  and  $m \in \mathbb{N}$  such that for  $M > m$  and  $i \in [N]$ ,  $\mathbb{P} - a.s.$*

$$\left| \widehat{\mathfrak{I}}_\Theta^M(U_{\psi,i}; Y^N | U_\psi^{i-1}) - \mathfrak{I}(U_{\psi,i}; Y^N | U_\psi^{i-1}) \right| < \varepsilon. \quad (24)$$

The proof of the theorem follows the consistency of the NPD in Theorem 3 and the triangle inequality.

*Proof.* For the proof we use Theorem 3 to claim that for every  $i \in [1 : N]$  we have the consistency of  $\mathfrak{H}_\Theta^M(U_i | U^{i-1})$  and  $\mathfrak{H}_\Theta^M(U_i | U^{i-1}, Y^N)$ . Hence, we have that for any  $\frac{\varepsilon}{2}$ ,  $\mathbb{P} - a.s.$

$$\begin{aligned} \left| \mathfrak{H}_\Theta^M(U_i | U^{i-1}, Y^N) - \mathfrak{H}(U_i | U^{i-1}, Y^N) \right| &< \frac{\varepsilon}{2}, \\ \left| \mathfrak{H}_\Theta^M(U_i | U^{i-1}) - \mathfrak{H}(U_i | U^{i-1}) \right| &< \frac{\varepsilon}{2}. \end{aligned}$$

Thus, due to the triangle inequality, we obtain that  $\mathbb{P} - a.s.$

$$\begin{aligned} \left| \widehat{\mathfrak{I}}_\Theta^M(U_{\psi,i}; Y^N | U_\psi^{i-1}) - \mathfrak{I}(U_{\psi,i}; Y^N | U_\psi^{i-1}) \right| &\leq \\ \left| \mathfrak{H}_\Theta^M(U_i | U^{i-1}) - \mathfrak{H}(U_i | U^{i-1}) \right| + \\ \left| \mathfrak{H}_\Theta^M(U_i | U^{i-1}, Y^N) - \mathfrak{H}(U_i | U^{i-1}, Y^N) \right| &< \frac{\varepsilon}{2} + \frac{\varepsilon}{2} = \varepsilon. \end{aligned} \quad \square$$

### C. Step 2: MI maximization

The maximization step involves fixing the parameter  $\theta^*$  obtained from the estimation step and maximizing  $\widehat{\mathfrak{I}}_\Theta^M(U_\psi^N; Y^N)$  w.r.t.  $\psi$ . The following theorem describes the gradient of  $\mathfrak{I}(U_\psi^N; Y^N)$  w.r.t.  $\psi$ .

**Theorem 5.** The gradient of  $I(U_\psi^N; Y^N)$  w.r.t.  $\psi$  is given by

$$\begin{aligned} \nabla_\psi I(U_\psi^N; Y^N) &= \\ &\mathbb{E}_{P_{X^N}^\psi \otimes W_{Y^N \| X^N}} \left[ \nabla_\psi \log P_{X^N}^\psi(X^N) Q(X^N, Y^N) \right], \end{aligned} \quad (25)$$

where  $Q(X^N, Y^N) = \log \frac{P_{U^N|Y^N}(X^N G_N | Y^N)}{P_{U^N}(X^N G_N)}$ .

Theorem 5 states that the gradients of the input distribution parameters  $\psi$  are computed via a re-parameterization trick [28], which allows for the computation of gradients through samples drawn from the joint distribution. The proof of Theorem 5 is given next.

*Proof.* Let  $Q(X^N, Y^N) = \log \frac{P_{U^N|Y^N}(X^N G_N | Y^N)}{P_{U^N}(X^N G_N)}$ . The gradient of  $I(U_\psi^N; Y^N)$  w.r.t.  $\psi$  is computed by the following steps:

$$\begin{aligned} \nabla_\psi I(U_\psi^N; Y^N) &= \nabla_\psi \sum_{x^N, y^N \in \mathcal{X}^N \times \mathcal{Y}^N} P_{X^N}^\psi(x^N) W_{Y^N \| X^N}(y^N \| x^N) Q(x^N, y^N) \\ &= \sum_{x^N, y^N \in \mathcal{X}^N \times \mathcal{Y}^N} \nabla_\psi P_{X^N}^\psi(x^N) W_{Y^N \| X^N}(y^N \| x^N) Q(x^N, y^N) \end{aligned}$$

---

**Algorithm 3** Code Rate Optimization via Neural Polar Decoders

---

**input:** Channel  $W$ , block length  $N$ , #iterations  $N_{\text{iters}}$ , #iterations of warm-up  $N_{\text{warm-up}}$ , learning rate  $\gamma$

**output:** Optimized  $\theta^*$ ,  $\psi^*$

---

Initiate the weights of  $\theta, \psi$

Generate  $\mathcal{D}_{M,N}^\psi \sim P_{X^N}^\psi \otimes W_{Y^N \| X^N}$

**Warm-up phase:**

**for**  $N_{\text{warm-up}}$  iterations **do**

    Sample  $x^N, y^N \sim \mathcal{D}_{M,N}^\psi$

    Update

$$\theta := \theta - \gamma \nabla_\theta [\mathcal{L}(x^N, y^N; \theta^{\text{ch}}) + \mathcal{L}(x^N, \mathbf{0}^N; \theta^{\text{co}})]$$

**end for**

**Main phase:**

**for**  $N_{\text{iters}}$  iterations **do**

    Sample  $x^N, y^N \sim \mathcal{D}_{M,N}^\psi$

**Maximization step:**

$$\text{Update } \psi := \psi + \gamma \nabla_\psi \widehat{I}_\theta(U_\psi^N; Y^N)$$

    Generate  $\mathcal{D}_{M,N}^\psi \sim P_{X^N}^\psi \otimes W_{Y^N \| X^N}$

**Estimation step:**

        Sample  $x^N, y^N \sim \mathcal{D}_{M,N}^\psi$

        Update

$$\theta := \theta - \gamma \nabla_\theta [\mathcal{L}(x^N, y^N; \theta^{\text{ch}}) + \mathcal{L}(x^N, \mathbf{0}^N; \theta^{\text{co}})]$$

**end for**

**return**  $\theta, \psi$

---

$$= \mathbb{E}_{P_{X^N}^\psi \otimes W_{Y^N \| X^N}} \left[ \nabla_\psi \log P_{X^N}^\psi(X^N) Q(X^N, Y^N) \right].$$

In the last equality, we multiplied and divided by  $P_{X^N}^\psi(x^N)$ , and used the fact the  $\frac{d}{dx} \log f(x) = \frac{\frac{d}{dx} f(x)}{f(x)}$ .  $\square$

Practically, the algorithm exploits the consistency of the NPDs to substitute  $\log \frac{P_{U^N|Y^N}(X^N G_N | Y^N)}{P_{U^N}(X^N G_N)}$  with  $\mathcal{L}(X^N, \mathbf{0}^N; \theta^{\text{co}}) - \mathcal{L}(X^N, Y^N; \theta^{\text{ch}})$  as plug-in estimator. Thus, given  $\theta^*$ , the gradients used to optimize  $\psi$  are given by:

$$\begin{aligned} \nabla_\psi \widehat{I}_{\theta^*}(U_\psi^N; Y^N) &= \mathbb{E}_{P_{X^N}^\psi \otimes W_{Y^N \| X^N}} \left[ \nabla_\psi \log P_{X^N}^\psi(X^N) \times \right. \\ &\quad \left. [\mathcal{L}(X^N, \mathbf{0}^N; \theta^{\text{co}}) - \mathcal{L}(X^N, Y^N; \theta^{\text{ch}})] \right]. \end{aligned} \quad (26)$$

#### D. Overall Algorithm

The overall algorithm integrates the two steps outlined in Sections IV-B, IV-C through an alternating maximization procedure. The algorithm begins with a “warm-up” phase, during which only step 1 is repeated. This initial phase focuses on estimating  $I(U_\psi^N; Y^N)$ , as its estimate is subsequently utilized as a proxy for  $\log \frac{P_{U^N|Y^N}}{P_{U^N}}$  in (25). Following the warm-up phase, step 1 and 2 are repeated interchangeably. The complete algorithm is detailed in Algorithm 3.

#### V. CAPACITY ESTIMATION AND CODE DESIGN

This section highlights the utility of NPDs in estimating channel capacity and designing codes with optimized code rates by applying Algorithm 3. It demonstrates the dual capabilities of the outcome of Algorithm 3 in addressing both tasks simultaneously. We present results for the Ising and Trapdoor channels, leveraging existing capacity bounds from the literature. Additionally, we use the SCT decoder

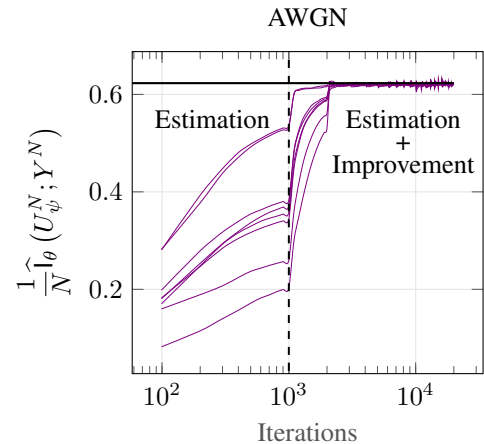


Figure 1: Evolution of  $I_\psi(U_\psi^N; Y^N)$  with respect to the iteration number of Algorithm 3 for the binary-input AWGN channel.

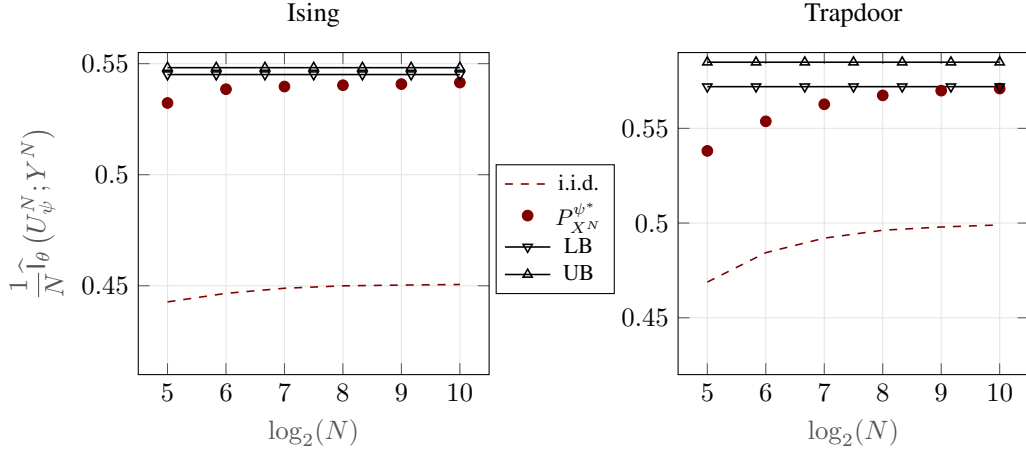


Figure 2: Estimated MI per symbol for the Ising and Trapdoor channels with various block lengths.

with i.i.d. uniform inputs to provide a theoretical benchmark for comparing with our algorithm. Sections V-A and V-B investigate the outcomes of Algorithm 3, focusing on the optimized input distribution with parameters  $\psi^*$  and the NPD with parameters  $\theta^*$ . Section V-A evaluates the estimated value of the optimized MI. Section V-B examines the BERs achieved by the optimized input distribution and NPD.

#### A. Capacity Estimation

The following experiments illustrate the MI attained by application of Algorithm 3 on the three instances of channels. For each of these channels, the estimated MI is recorded, as given in Equation (23). Figure 1 illustrates the results obtained on the binary-input AWGN channel. It illustrates the evolution of the estimated MI throughout the iterations of the algorithm. It is visible that the estimated MI values converge to the optimal MI for the binary-input AWGN channel. The figure presents results from 10 independent simulations, each initialized with a randomly chosen value for  $\psi := P_X(1)$  within the interval  $[0, 1]$ . Algorithm 3 is executed with  $N_{\text{warmup}} = 1000$ , and

therefore, during the initial  $N_{\text{warmup}}$  iterations,  $\psi$  is fixed. After  $N_{\text{warmup}}$  iterations, the algorithm starts optimizing  $\psi$ . Notably, after approximately 2000 iterations, the algorithm converges to the optimal value of  $I(X; Y)$  for  $P_X(1) = 0.5$ .

Figure 2 illustrates the results for the Ising and Trapdoor channels [29]. This experiment showcases the estimated value  $\frac{1}{N} \hat{I}_\theta(U^N; Y^N)$  obtained upon termination of Algorithm 3 for various block lengths  $N = 2^n$ . The solid red circles show the empirical MI values for the optimized input distribution,  $P_{X^N}^{\psi^*}$ . The benchmarks for comparison in this experiment is lower and upper bounds on the capacity of the Ising channel and Trapdoor channels. The bounds are given by  $0.5451 \leq C_{\text{Ising}} \leq 0.5482$ , as derived in [21], [30], and by  $0.572 \leq C_{\text{Trapdoor}} \leq 0.5849$ , as derived in [21], [31]. The results demonstrate that as  $N$  increases,  $\frac{1}{N} \hat{I}_\theta(U^N; Y^N)$  converges toward the true value of the channel capacity. In order to emphasize the improvement of the optimized input distribution over a uniform i.i.d. input distribution, we plotted the empirical MI attained by the SCT decoder. For the Ising channel, the optimized input distribution achieves MI of 0.5415, compared to 0.45 for the uniform i.i.d. input.

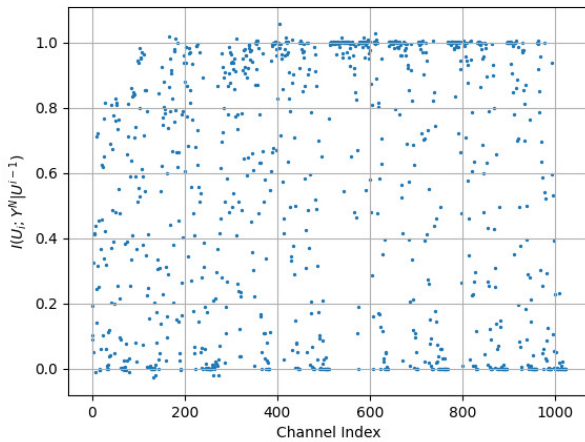


Figure 3: Polarization for the Ising channel with optimized input distribution.

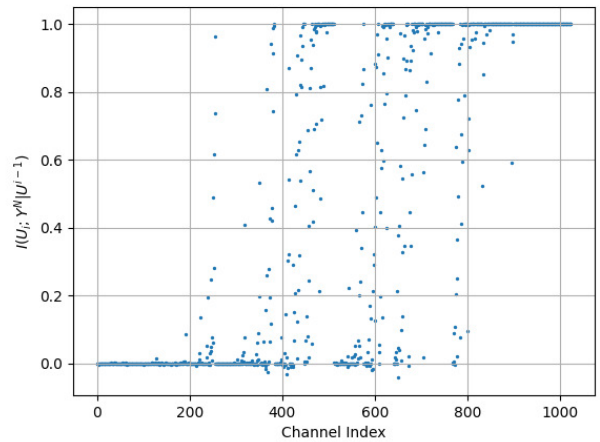


Figure 4: Polarization for the Ising channel with uniform i.i.d. input distribution.

Similarly, for the Trapdoor channel, the optimized distribution attains MI of 0.571, whereas the uniform i.i.d. input yields 0.5.

Figures 3 and 4 illustrate the polarization of the synthetic channels for the Ising channel with optimized input distribution and uniform i.i.d. input distribution, respectively. The figure shows that the optimized input distribution increases the average MI of the synthetic channels on the expense of the polarization of the synthetic channels. This presents a drawback when build polar codes with the optimized input distribution, as discussed in Section V-B.

### B. Channel Coding

This section describes how the output of Algorithm 3 is utilized to construct a polar code. At this stage, the parameters  $\theta^* = \{\theta^{*,\text{co}}, \theta^{*,\text{ch}}\}$  and  $\psi^*$  are fixed and employed for code design, encoding, and decoding. During the code design phase, the frozen set  $\mathcal{F}$  is determined. After this step, the parameters  $\psi^*$  are discarded, and only  $\theta^*$  is used by the encoder and decoder. This is because the encoding uses the HY scheme, which relies on the NPD parameterized by  $\theta^{*,\text{co}}$ , which, after optimization, approximates the distribution defined by  $\psi^*$ .

As illustrated in Figures 3 and 4, the optimized input distribution reduces the polarization of the synthetic channels. This reduction necessitates additional coding to map the information bits onto  $U_{\mathcal{A}}$ . This issue was previously identified in [24], [32], where methods such as homophonic coding and arithmetic coding were proposed to address it. In this work, we propose using an adaptive frozen set to mitigate this issue. The remainder of this section outlines the implementation of the key components for polar codes: code design, encoding, and decoding.

1) **Code Design:** The code design involves estimating the MI of the synthetic channels. For this purpose, we extend Algorithm 1 to return  $\mathbf{v}_n, \mathbf{l}_n$  instead of  $\mathcal{L}(x^N, y^N; \theta)$ . Recall that  $\mathbf{v}_n = u^N$  and  $\mathbf{l}_n$  is the estimated LLRs

$\{L_{U_i|Y^N, U^{i-1}}(y^N, u^{i-1})\}_{i=1}^N$ . Let the extension of Algorithm 1 be denoted by

$$[\mathbf{v}_n, \mathbf{l}_n] = \widetilde{\text{Alg}}_1(x^N, y^N; \theta'), \quad (27)$$

where  $\theta' = \theta^{*,\text{co}}$  or  $\theta' = \theta^{*,\text{ch}}$ . With this notation, the code design is described by the following steps. First, we generate  $\mathcal{D}_{M,N}^{\psi^*} \sim P_{X^N}^{\psi^*} \otimes W_{Y^N|X^N}$ . Next, for every  $x^N, y^N \in \mathcal{D}_{M,N}^{\psi^*}$ , we compute

$$[\mathbf{v}_n^{\text{co}}, \mathbf{l}_n^{\text{co}}] = \widetilde{\text{Alg}}_1(x^N, \mathbf{0}^N; \theta^{*,\text{co}}) \quad (28)$$

$$[\mathbf{v}_n^{\text{ch}}, \mathbf{l}_n^{\text{ch}}] = \widetilde{\text{Alg}}_1(x^N, y^N; \theta^{*,\text{ch}}). \quad (29)$$

Then, the empirical MI of the synthetic channels is computed for all  $i \in [1 : N]$

$$\begin{aligned} \widehat{\mathbf{l}}_{\theta^*}(U_i; Y^N | U^{i-1}) = & \quad (30) \\ & \frac{1}{M} \sum_{x^N, y^N \in \mathcal{D}_{M,N}^{\psi^*}} \left[ -v_{n,i}^{\text{co}} \log \sigma(l_{n,i}^{\text{co}}) - (1 - v_{n,i}^{\text{co}}) \log(1 - \sigma(l_{n,i}^{\text{co}})) \right] \\ & - \left[ -v_{n,i}^{\text{ch}} \log \sigma(l_{n,i}^{\text{ch}}) - (1 - v_{n,i}^{\text{ch}}) \log(1 - \sigma(l_{n,i}^{\text{ch}})) \right]. \quad (31) \end{aligned}$$

Given the design rate  $R \in [0, 1]$ , we set the information set  $\mathcal{A}$  to include the indices with the highest  $k = \lfloor RN \rfloor$  values of  $\widehat{\mathbf{l}}_{\theta^*}(U_i; Y^N | U^{i-1})$  and the frozen set, implied by  $\mathcal{F} = [1 : N] \setminus \mathcal{A}$ .

2) **Encoder with Fixed Frozen Set:** Let  $b^k$  be uniform i.i.d. information bits and let  $\mathcal{F} \subset [1 : N]$  be the frozen set. In order to encode  $b^k$  into  $x^N$ , the encoder uses the recursive formulas of the SC decoding of the NPD with the parameters  $\theta^{*,\text{co}}$ . That is, the encoder uses the constant channel embedding to compute the LLRs  $\{L_{U_i|U^{i-1}}^{\theta^{*,\text{co}}}(u^{i-1})\}_{i=1}^N$  sequentially. The only difference is what happens when the decoder reaches the decision stage. Here, the encoder assigns an information bit or decides on the value of the frozen bits. Thus, upon reaching the  $i^{\text{th}}$  decision

$$u_i = \begin{cases} \text{sgn} \left( L_{U_i|U^{i-1}}^{\theta^{*,\text{co}}}(u^{i-1}) \right) & i \in \mathcal{F} \\ b_{j(i)} & i \in \mathcal{A}, \end{cases} \quad (32)$$

where  $j(i) = |\{l \in \mathcal{A} : l \leq i\}|$  and  $\text{sgn}$  is the sign function.

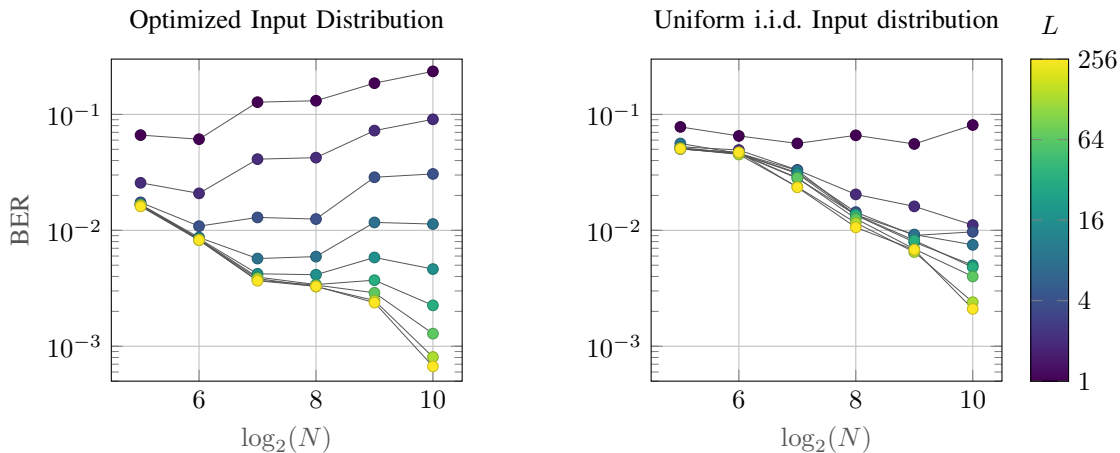


Figure 5: Comparison of the BERs attained by the outcome of Algorithm 3 (left) and by the SCT decoder with uniform i.i.d. input distribution (right) on the Ising channel. The decoding is done by SCL with values of  $L = \{1, 2, 4, 8, 16, 32, 64, 128, 256\}$ .

3) **Encoder with Adaptive Frozen Set:** Let  $b_1, b_2, \dots$  be information bits the encoder needs to transmit across multiple blocks. An encoder with an adaptive frozen set operates similarly to one with a fixed frozen set, but it allows for the frozen positions to vary from block to block. Specifically, the encoder decides whether to place an information bit or a shaping bit in each position  $i \in \mathcal{A}$  by inspecting the LLR  $L_{U_i|U^{i-1}}^{\theta^*, \text{co}}(u^{i-1})$ . If the LLR is close to 0, it indicates that  $P_{U_i|U^{i-1}}^{\theta^*, \text{co}}(\cdot|u^{i-1})$  is approximately uniform, and an information bit can be inserted without distorting the codeword distribution from the optimized one. Conversely, if the LLR is large in magnitude, the conditional distribution is biased, and inserting an information bit would shift the codeword distribution. In such cases, the encoder inserts a shaping bit sampled according to  $P_{U_i|U^{i-1}}$ . We define the adaptive frozen set

$$\mathcal{F}_d = \{i \in [1 : N] : i \in \mathcal{F} \text{ or } |L_{U_i|U^{i-1}}^{\theta^*, \text{co}}(u^{i-1})| > t\}, \quad (33)$$

and accordingly,  $\mathcal{A}_d = [N] \setminus \mathcal{F}_d$ , where  $t > 0$  is a predetermined threshold. The code rate in this setting is computed by  $\mathbb{E}[|\mathcal{A}_d|]/N$ .

4) **Decoder:** The decoder observes  $y^N$  and uses the parameters  $\theta^*, \text{co}, \theta^*, \text{ch}$  to decode  $u^N$ . This amounts to apply SC decoding of the NPD with the parameters  $\theta^*, \text{co}, \theta^*, \text{ch}$  simultaneously. That is, the decoder uses both embeddings to compute the LLRs  $\{L_{U_i|U^{i-1}}^{\theta^*, \text{co}}(u^{i-1})\}_{i=1}^N$  and  $\{L_{U_i|Y^N, U^{i-1}}^{\theta^*, \text{ch}}(y^N, u^{i-1})\}_{i=1}^N$ . Upon reaching the decision stage, the decoder makes its decision according to the following rule

$$\hat{u}_i = \begin{cases} \text{sgn} \left( L_{U_i|U^{i-1}}^{\theta^*, \text{co}}(\hat{u}^{i-1}) \right) & i \in \mathcal{F} \\ \text{sgn} \left( L_{U_i|Y^N, U^{i-1}}^{\theta^*, \text{ch}}(y^N, \hat{u}^{i-1}) \right) & i \in \mathcal{A}. \end{cases} \quad (34)$$

In the adaptive frozen set setting, since the decoder computes also  $L_{U_i|U^{i-1}}(u^{i-1})$ , it can also determine the adaptive frozen set  $\mathcal{F}_d$ . A block error is declared if  $\hat{u}_i \neq u_i$  for any  $i \in \mathcal{A}_d$  or the decoder fails to discover the information set  $\mathcal{A}_d$ .

5) **Experiments:** The following experiments illustrate the incurred BERs of SCL decoding for various list size  $L = \{1, 2, 4, 8, 16, 32, 64, 128, 256\}$  ( $L = 1$  is SC decoding) on the Ising channel. The experiments compare the attained BERs by a uniform i.i.d. input distribution and SCT list decoder, which provides a theoretical benchmark, and the BERs attained by SCL decoding of the NPD with parameter  $\theta^*$ , as obtained by Algorithm 3.

Figure 5 illustrates the decoding errors for the Ising channel for the case where the bits on the information set distribute according to  $P_{U_i|U^{i-1}}^{\theta^*, \text{co}}(\cdot|u^{i-1})$ . The goal of this experiment is to examine the benefit of optimizing the input distribution when there is no rate loss when encoding information bits on  $\mathcal{A}$ . For the optimized input distribution, the size of the information was set to  $\lfloor 0.4N \rfloor$ . Since the optimized input distribution is not necessarily uniform, the sum of conditional entropies  $\sum_{i \in \mathcal{A}} \mathbb{H}(P_{U_i|U^{i-1}}^{\theta^*, \text{co}})$  may be strictly less than  $0.4N$ . Hence, to make a fair comparison between uniform and optimized input distribution, we set the code rate of uniform and i.i.d. input distribution to be  $\frac{1}{N} \sum_{i \in \mathcal{A}} \mathbb{H}(P_{U_i|U^{i-1}}^{\theta^*, \text{co}})$ . Figure 5 shows the optimized input distribution attains lower BERs for code rate of 0.4 for the optimized input distribution and approximately 0.37 for the i.i.d. inputs.

Figure 6 shows the frame error rates (FERs) for the Ising channel when using adaptive frozen sets. In this experiment the uniform input distribution uses code rate of 0.4 and the optimized input distribution uses code rate of 0.435 and threshold 1, which yielded an expected rate of 0.4. Under this setting we observe better performance of the optimized input distribution than the uniform and i.i.d. input distribution.

Since  $R$  is close to the MI, we observe non-monotonic behavior in the BER as a function of block length, particularly for small list sizes. In these cases, increasing the block length leads to performance degradation due to the limitations of the SC decoder at moderate block lengths. This phenomenon is observed not only for the NPD, but also for the SCT

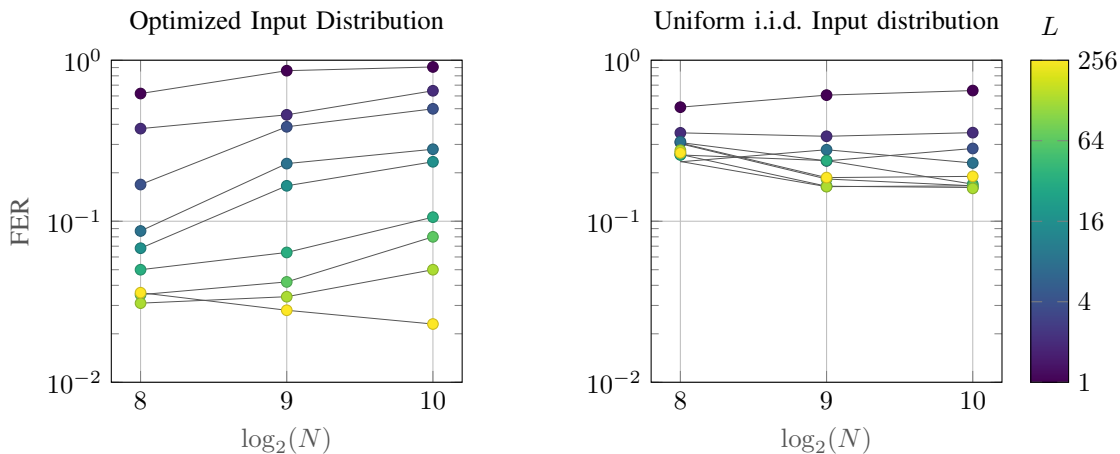


Figure 6: Comparison of the FERs attained by the outcome of Algorithm 3 (left) and by the SCT decoder with uniform i.i.d. input distribution (right) on the Ising channel. The optimized input distribution uses adaptive frozen set with  $t = 1$ . The decoding is done by SCL with values of  $L = \{1, 2, 4, 8, 16, 32, 64, 128, 256\}$

decoder, which leverages the channel model to compute exact posteriors of the synthetic channels. This further supports the interpretation that the degradation arises from inherent limitations of the SC decoding principle rather than the specific decoder implementation.

## VI. CONCLUSIONS AND FUTURE WORK

In this paper, we proposed a novel method to optimize the input distribution of polar codes using NPDs. Our approach addresses the dual challenges of maximizing code rates over input distributions and providing a practical coding scheme within the framework of polar codes. This is particularly valuable for scenarios where the channel model is unknown, treating the channel as a black-box that generates output samples from input samples.

The methodology involves a two-phase process: a training phase and an inference phase. During the training phase, we alternate between estimating MI using NPDs and optimizing the input distribution parameters. In the inference phase, the optimized model is used to construct polar codes, incorporating the HY scheme and list decoding to enhance performance.

Our experimental results on memoryless channels and FSCs demonstrated the effectiveness of our approach. We observed significant improvements in MI and BERs compared to uniform and i.i.d. input distributions, validating our method for block lengths up to 1024. The scalability of our approach suggests its potential applicability to real-world communication systems, bridging the gap between theoretical capacity estimation and practical coding performance.

Future work will focus on mitigating the reduced polarization caused by optimized inputs by developing techniques that improve code rates without compromising the polarization of synthetic channels.

Overall, our work contributes to advancing the understanding and application of NPDs in channel coding, providing a robust framework for high-performance communication systems. Future research directions include exploring further optimizations and extensions of our methodology to other types of channels and coding schemes.

## REFERENCES

- [1] Z. Aharoni, B. Huleihel, H. D. Pfister, and H. H. Permuter, "Code Rate Optimization via Neural Polar Decoders," in *2024 IEEE International Symposium on Information Theory (ISIT)*, 2024, pp. 2424–2429.
- [2] R. Blahut, "Computation of channel capacity and rate-distortion functions," *IEEE transactions on Information Theory*, vol. 18, no. 4, pp. 460–473, 1972.
- [3] S. Arimoto, "An algorithm for computing the capacity of arbitrary discrete memoryless channels," *IEEE Transactions on Information Theory*, vol. 18, no. 1, pp. 14–20, 1972.
- [4] P. Vontobel, A. Kavcic, and D. Arnold, "A generalization of the Blahut-Arimoto algorithm to finite-state channels," *IEEE Trans. Inf. Theory*, vol. 54, no. 5, pp. 1887–1918, 2008.
- [5] I. Naiss and H. H. Permuter, "Extension of the blahut–arimoto algorithm for maximizing directed information," *IEEE Transactions on Information Theory*, vol. 59, no. 1, pp. 204–222, 2012.
- [6] S. Tatikonda and S. Mitter, "The capacity of channels with feedback," *IEEE Trans. Inf. Theory*, vol. 55, no. 1, pp. 323–349, 2009.
- [7] H. H. Permuter, P. Cuff, B. V. Roy, and T. Weissman, "Capacity of the trapdoor channel with feedback," *IEEE Trans. Inf. Theory*, vol. 54, no. 7, pp. 3150–3165, 2009.
- [8] J. Jiao, H. H. Permuter, L. Zhao, and T. Weissman, "Universal estimation of directed information," *IEEE Trans. Inf. Theory*, vol. 59, no. 10, pp. 6220–6242, 2013.
- [9] O. Elishco and H. H. Permuter, "Capacity and coding for the Ising channel with feedback," *IEEE Trans. Inf. Theory*, vol. 60, no. 9, pp. 5138–5149, 2014.
- [10] J. Massey, "Causality, feedback and directed information," *Proc. Int. Symp. Inf. Theory Applic. (ISITA-90)*, pp. 303–305, 1990.
- [11] Z. Aharoni, D. Tsur, Z. Goldfeld, and H. Permuter, "Capacity estimation using machine learning," in *Machine Learning and Wireless Communication*, A. Goldsmith, D. Gunduz, H. V. Poor, and Y. C. Eldar, Eds. The address of the publisher: Cambridge University Press, 02.
- [12] D. Tsur, Z. Aharoni, Z. Goldfeld, and H. Permuter, "Neural estimation and optimization of directed information over continuous spaces," *IEEE Trans. Inf. Theory*, 2023.
- [13] —, "Data-driven optimization of directed information over discrete alphabets," *IEEE Trans. Inf. Theory*, 2023.
- [14] N. A. Letizia and A. M. Tonello, "Discriminative Mutual Information Estimation for the Design of Channel Capacity Driven Autoencoders," in *2022 International Balkan Conference on Communications and Networking (BalkanCom)*, 2022, pp. 41–45.
- [15] Z. Li, R. She, P. Fan, C. Peng, and K. B. Letaief, "Learning Channel Capacity With Neural Mutual Information Estimator Based on Message Importance Measure," *IEEE Transactions on Communications*, vol. 72, no. 3, pp. 1370–1384, 2024.
- [16] E. Arikan, "Channel polarization: A method for constructing capacity-achieving codes for symmetric binary-input memoryless channels," *IEEE Trans. Inf. Theory*, vol. 55, no. 7, pp. 3051–3073, 2009.
- [17] I. Tal and A. Vardy, "List decoding of polar codes," *IEEE Trans. Inf. Theory*, vol. 61, no. 5, pp. 2213–2226, 2015.
- [18] 3rd Generation Partnership Project (3GPP), "Technical specification group radio access network; nr; multiplexing and channel coding," 3GPP, Tech. Rep. 3GPP TS 38.212 version 16.5.0, March 2021.
- [19] Z. Aharoni, B. Huleihel, H. D. Pfister, and H. H. Permuter, "Data-driven neural polar codes for unknown channels with and without memory," *arXiv preprint arXiv:2309.03148*, 2023.
- [20] J. Honda and H. Yamamoto, "Polar coding without alphabet extension for asymmetric models," *IEEE Trans. Inf. Theory*, vol. 59, no. 12, pp. 7829–7838, 2013.
- [21] B. Huleihel, O. Sabag, H. H. Permuter, N. Kashyap, and S. Shamai, "Computable upper bounds on the capacity of finite-state channels," *IEEE Trans. Inf. Theory*, 2021.
- [22] G. Kramer, *Directed Information for Channels with Feedback*, 1998, vol. 11.
- [23] A. M. Fer and H. G. Zimmermann, "Recurrent neural networks are universal approximators," in *Proceedings of International Conference on Artificial Neural Networks*. Springer, 2006, pp. 632–640.
- [24] R. Wang, J. Honda, H. Yamamoto, R. Liu, and Y. Hou, "Construction of polar codes for channels with memory," in *2015 IEEE Information Theory Workshop-Fall (ITW)*. IEEE, 2015, pp. 187–191.
- [25] E. Ising, "Beitrag zur theorie des ferromagnetismus," *Zeitschrift für Physik*, vol. 31, no. 1, pp. 253–258, 1925.
- [26] D. Blackwell, "Information theory," in *Modern Mathematics for the Engineer: Second Series*. New York, NY, USA: Dover, 1961, pp. 182–193.
- [27] S. Hochreiter, "Long short-term memory," *Neural computation*, vol. 9, no. 8, pp. 1735–1780, 1997.
- [28] J. Schulman, N. Heess, T. Weber, and P. Abbeel, "Gradient estimation using stochastic computation graphs," *Advances in neural information processing systems*, vol. 28, 2015.
- [29] T. Berger and F. Bonomi, "Capacity and zero-error capacity of Ising channels," *IEEE Trans. Inf. Theory*, vol. 36, pp. 173–180, 1990.
- [30] A. Sharov and R. Roth, "On the capacity of generalized ising channels," in *Proc. IEEE Int. Symp. Inf. Theory (ISIT)*, 2015, pp. 2256–2260.
- [31] K. Kobayashi, H. Morita, and M. Hoshi, "Some considerations on the trapdoor channel," in *Proceedings of the 3rd Asian-European Workshop on Information Theory*, 2003, pp. 9–10.
- [32] R. Wang, J. Honda, H. Yamamoto, and R. Liu, "FV polar coding for lossy compression with an improved exponent," in *2015 IEEE International Symposium on Information Theory (ISIT)*, 2015, pp. 1517–1521.